THz Hot-Electron Micro-Bolometer Based on Low-Mobility 2-DEG in GaN Heterostructure

Jae Kyu Choi, Vladimir Mitin, *Fellow, IEEE*, Rahul Ramaswamy, Victor A. Pogrebnyak, Mehdi P. Pakmehr, Andrey Muravjov, Michael S. Shur, *Fellow, IEEE*, John Gill, Imran Mehdi, *Fellow, IEEE*, Boris S. Karasik, *Member, IEEE*, and Andrei V. Sergeev

***Abstract*— We present the results on design, fabrication, and characterization of a hot-electron bolometer based on low-mobility 2-D electron gas (2-DEG) in an AlGaN/GaN heterostructure. The characterization of our hot-electron bolometers demonstrates that the following can be achieved simultaneously: 1) strong coupling to incident THz radiation due to strong Drude absorption; 2) significant THz heating of 2-DEG due to the small value of the electron heat capacity; and 3) high responsivity due to the strong temperature dependence of 2-DEG resistance. Low contact resistance achieved in our devices ensures that THz radiation couples primarily to the 2-DEG. Due to a small electron momentum relaxation time, the real part of the 2-DEG sensor impedance is ∼50–100 Ω, which provides good impedance matching between sensors and antennas. The room temperature responsivity of our devices reaches ∼0.04 A/W at 2.55 THz along with a noise equivalent power of ∼5 nW/Hz$^{1/2}$.**

***Index Terms*— AlGaN/GaN heterostructure, THz hot electron bolometer, 2-D electron gas (2-DEG).**

I. Introduction

THz detectors are critically important for a number of applications related to chemical and biological sensing. THz systems are considered the top candidate for atmospheric remote sensing, monitoring wide-area public and industrial facilities, as well as detection of toxic industrial chemicals, chemical agents, and explosives [1]. The THz sensing is also an attractive for screening personnel and hand held materials because of its ability to detect the composition, size, and shape of the materials using transmission and reflection characteristics with spectral resolution.

Modern micro- and nanotechnologies provide a variety of possibilities for qualitative improvement of conventional detectors and development of novel devices. Recently, the significant progress has been achieved in developing the quantum THz detectors based on novel nanomaterials, such as quantum dots [2], quantum nano wires [3], quantum well (QW) structures [4], carbon nanotubes [5], and graphene [6], [7]. These structures were fabricated using the modern nanoscale band-structure engineering, and their operation is based on electron transitions between localized and conducting states at THz frequency. Sensitivity of the QW detectors is determined by the spacing between quantum levels, their width, and generation-recombination processes.

However, all quantum THz detectors have one unavoidable drawback - a low radiation hardness that imposes a significant limitation on applications of these detectors in aeronautic and space missions.

In spite of the progress in quantum detectors, bolometers still remain to be "working horses" for many THz applications. They are widely used both as direct and heterodyne detectors. Hot-electron bolometers (devices based on electron heating) usually offer a better combination of sensitivity and speed. Recent improvements in the hot-electron bolometers [8], [9] show great promise of these devices for advanced quantum technologies, such as quantum calorimetry and photon counting [10].

There are many research groups developing THz sensing technologies based on direct detection. Compared to heterodyne detection, the receivers with direct detection can achieve the highest sensitivity limited only by the power fluctuation in the signal. However, direct detection destroys information about the phase of the THz signal that is crucial for many applications [11]–[13]. In THz spectroscopy, a heterodyne receiver enables sampling of a large number of spectrum channels simultaneously, while in direct detection only one channel at a time is analyzed. In this way, heterodyne sensing drastically reduces the data acquisition time and significantly improves the resolution [11]. While there is an urgent need for compact THz receivers, the available heterodyne systems are still too expensive and bulky. Available

Manuscript received June 27, 2012; revised September 13, 2012; accepted October 2, 2012. Date of publication October 12, 2012; date of current version December 6, 2012. This work was supported in part by the National Science Foundation's DMR program under Grant 0907126 and the National Aeronautics and Space Administration (NASA) SBIR under Grant NNX12CE53P (2011). This work was carried out in part at the Jet Propulsion Laboratory, California Institute of Technology, under a contract with NASA. The associate editor coordinating the review of this paper and approving it for publication was Dr. Francis P. Hindle. *(Corresponding author: V. A. Pogrebnyak.)*

J. K. Choi, V. Mitin, R. Ramaswamy, V. A. Pogrebnyak, and A. V. Sergeev are with the Department of Electrical Engineering, University at Buffalo, State University of New York, Buffalo, NY 14260 USA (e-mail: jkchoi2@buffalo.edu; vmitin@buffalo.edu; stn.rahul@gmail.com; vp23@buffalo.edu; asergeev@buffalo.edu).

M. P. Pakmehr is with the Department of Physics, University at Buffalo, Buffalo, NY 14260 USA (e-mail: mpakmehr@buffalo.edu).

A. Muravjov and M. S. Shur are with the Department of Electrical and Computer Engineering, Rensselaer Polytechnic Institute, Troy, NY 12180 USA (e-mail: amuravie@gmail.com; shurm@rpi.edu).

J. Gill, I. Mehdi, and B. S. Karasik are with the Jet Propulsion Laboratory, California Institute of Technology, 4800 Oak Grove Drive, Pasadena, CA 91109 USA (e-mail: john.j.gill@jpl.nasa.gov; Imran.Mehdi@jpl.nasa.gov; boris.s.karasik@jpl.nasa.gov).

Color versions of one or more of the figures in this paper are available online at http://ieeexplore.ieee.org.

Digital Object Identifier 10.1109/JSEN.2012.2224334

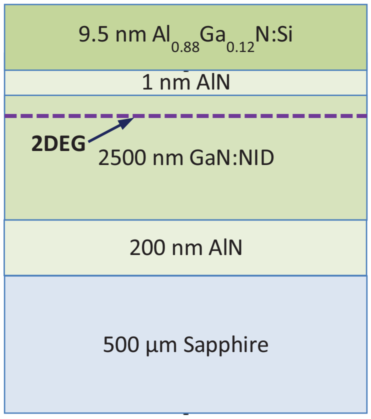

Fig. 1. Diagram of the AlGaN/GaN heterostructure with 2-DEG.

now receivers, based on Schottky diodes [14]–[16] and operating at room temperature, require large powerful lasers.

The receivers based on superconducting hot-electron bolometers and operating at helium temperatures require cryorefrigeration which is often unaffordable [17]–[20].

Hot-electron bolometers based on nanostructures allow for a significant reduction of the electron heat capacity, which in turn improves two critical for THz heterodyne sensing parameters: the noise caused by fluctuations of the electron energy (temperature) and power of a local oscillator. Recently, such bolometers have attracted significant interest due to the development of quantum cascade lasers [21], [22], which can be integrated with semiconductor hot-electron bolometers on the same chip [23].

A two-dimensional electron gas in semiconductor heterostructures was identified as a promising medium for hot-electron bolometers in early 90 s [24]. So far the research has been mainly limited by the sub-THz range where 2-DEG AlGaAs/GaAs HEBs demonstrated a good performance [25]–[27]. However, above ∼0.5 THz, the performance of the AlGaAs/GaAs detectors drastically deteriorates because the conductivity of 2-DEG in aAlGaAs/GaAsheterostructure becomes highly inductive at this frequency that significantly reduces coupling to the THz radiation. One of the approaches for improvement of the coupling at THz frequencies is based on the use of plasmonic semiconductor structures, where THz radiation excites the plasma modes which transfer THz energy to the electron subsystem [28]–[30].

Our approach to improving the coupling between THz radiation and 2-DEG is based on enhancing the THz Drude absorption by introducing additional disorder into heterostructure material [31]. In a semiconductor heterostructure, the disorder can be introduced by impurities, defects, and interface roughness, which increase the scattering of 2D electrons by the random potential. The disorder can be controlled during the heterostructure growth. Our heterostructures have a significant interface lateral disorder that increases the elastic electron scattering and reduces the electron momentum relaxation time. As a result, the disordered heterostructures provides a strong coupling to the THz radiation via the Drude absorption. GaN heterostructures are characterized by a strong inelastic electron-phonon scattering, which increases due to disorder [32]. This energy relaxation mechanism provides fast cooling of hot electrons, therefore a short detector operating time and wide frequency bandwidth for heterodyne operation. Finally, a high responsivity and low noise in the hot-electron detectors are achieved due to a small electron heat capacity.

In our devices,a small heat capacity is realized due to the low dimensionality of the electron subsystem and micro-patterning. In this work, we also investigate different approaches for coupling between 2-DEG sensors and planar antennas. Our AlGaN/GaN heterostructures have a 2-DEG sheet resistance ∼250 Ω. This allows to employ conventional THz antennas with an impedance of ∼50–100 Ω (see Section II).

II. Fabrication and Characterization of a GaN Heterostructure

A. Wafer Growth and Device Processing

GaN heterostructures have a number of optoelectronic applications [33]–[35]. GaN is an III-V direct band gap semiconductor that is very hard and has a Wurtzite crystal structure with a 3.4 eV band gap. GaN has a large electron effective mass ($m^* = 0.2\ m_0$) and a large longitudinal optical (LO) phonon energy ($E_{LO} = 90$ meV). It is important that GaN has a high thermal conductivity (1.3 W/cm K) which allows to avoid overheating of the device at high operating temperature [36]. Compared to the 2-DEG in AlGaAs/GaAs ($\sim 3\ \times 10^{11}$ cm^{-2}), the AlGaN/GaN heterostructures have a significantly greater carrier concentration at the interface, n $\sim 10^{13}$ cm^{-2}. This is mainly due to the piezoelectric polarization of the strained top layer, which is five times larger than in similar AlGaAs/GaAs structures [37].

Many important applications of GaN are based on heterostructures with a high mobility 2-DEG. As it was highlighted above, the strong coupling to THz radiation and hence significant heating of 2-DEG require a low electron mobility i.e. a short electron mean free path. From the other side, for the impedance matching between a 2-DEG structure and a typical 50–100 Ω antenna or read-out circuit, the resistance of the 2-DEG should be decreased to ∼100 Ω/□. We could meet these conditions by increasing a 2-DEG concentration to 10^{13} cm^{-2}.

The AlGaN/GaN heterostructures used in this work were grown on two-inch (0001) sapphire substrates using the migration enhanced metal-organic chemical vapor deposition (MEMOCVD) technique. First, a 200 nm undoped AlN layer was grown to control the surface roughness on the sapphire substrate from propagating upward and also to control a density of the dislocations caused by the lattice mismatch between the upper GaN layer and the sapphire. Following this, a 2.5 μm non-intentionally doped GaN buffer layer was grown. Then a 1 nm AlN spacer layer and a 10 nm Si-doped $Al_{0.88}Ga_{0.12}N$ top layer were deposited. Finally, the samples were covered with SiO_2 to avoid oxidation of Al present in the top layer. Several wafers with different level of disorder were grown for manufacturing our devices. The AlGaN/GaN wafer structure used for fabrication of the THz HEBs is shown in Fig. 1.

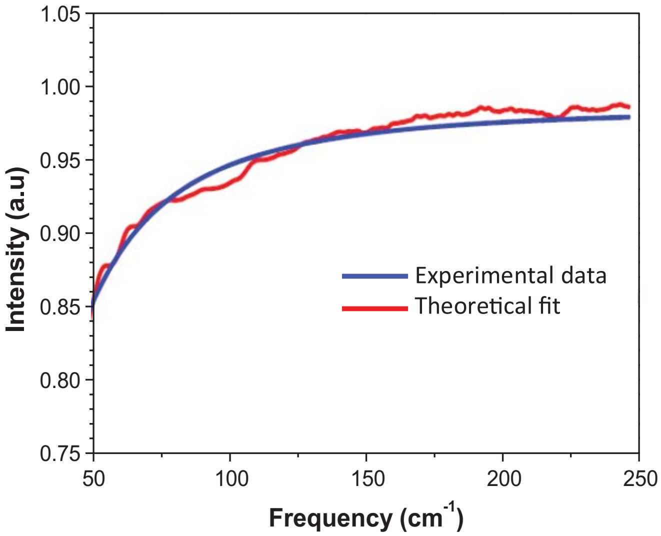

Fig. 2. THz transmission versus frequency for 2-DEG layer. The red curve (not smooth) represents the experimental data, while the blue curve (smooth) represents the theoretical fit.

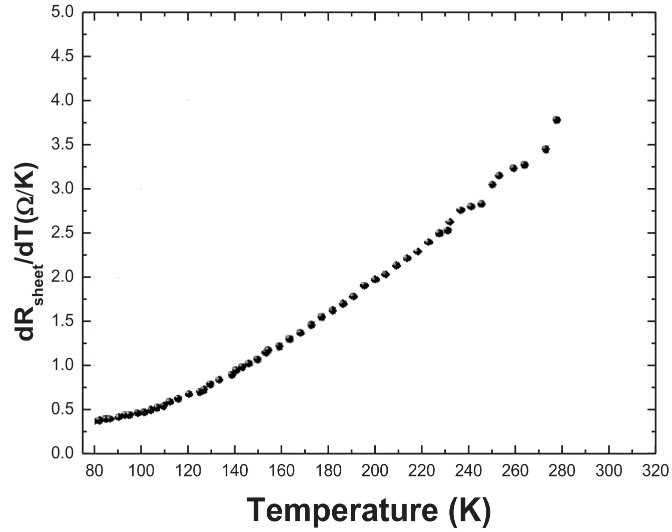

Fig. 3. Temperature coefficient dR/dT of the 2-DEG resistance as a function of the lattice temperature.

The room temperature electron mobility, μ, electron concentration, n, and sheet resistance, R, were determined using the Hall and Van-der-Paw techniques: $\mu = 2400$ cm^2/Vs, n $= 1 \times 10^{13}$ cm^{-2}, and $R = 248$ Ω/□. Such sheet resistance is convenient for fabrication of THz devices with ∼50–70 Ω impedance required for impedance matching between the 2-DEG channel, antenna and a transmission line. The impedance matching was achieved in each specific device by varying the 2-DEG channel geometry (length and width), shape of the mesa, and the antenna configuration.

B. Ohmic Contacts Characterization

The Transfer Line Method (TLM) was employed to measure the contact and sheet resistance of the fabricated devices. The TLM pattern was defined onto a rectangular mesa by the standard lift-off technique to form a series of seven $150 \times 50\ \mu\text{m}^2$ contacts with an increasing channel separation of 2, 4, 6, 8, 10, and 12 μm. The samples were rapidly annealed at 850 °C to minimize the contact resistance. The minimal contact resistance achieved at room temperature was 0.34 Ω mm. After fabrication, current-voltage characteristics of the devices were measured. The symmetric Ohm's law plots confirmed good quality of the contacts.

C. Optical Characterizations

The transmission measurement was performed using a Bruker IFS 66V/S FTIR spectrometer at room temperature. A helium cooled Si bolometer was used with a 370 cm^{-1} input low-pass filter. A conventional glow-bar light emitter in the FTIR system was used as the source. The 2-DEG sample was mounted in a cryostat. The whole setup was evacuated to reduce the water absorption in the beam path. The results of the THz characterization are presented in Fig. 2. Fig. 2 shows the transmission of THz radiation through the 2-DEG in the GaN heterostructure. The 2-DEG transmission was determined by subtraction of the substrate transmission from the transmission spectrum of the whole structure, which were measured separately. As it is seen from Fig. 2, the experimental data are well fitted by the Drude model, where the transmission coefficient, T, is given by [38]:

$$T(\omega) = 1 - \frac{1 - T_0}{1 + T_0(\omega\tau)^2}, \qquad T_0 = \frac{x^2}{(1+x)^2}, \quad x = \frac{2R_0}{Z_0} \quad (1)$$

where T_0 is the transmission at frequencies far below the inverse momentum relaxation time τ (i.e. at $\omega\tau << 1$), R_0 is the DC sheet resistance of 2-DEG, ω is the angular frequency of THz radiation, Z_0 is the impedance of vacuum, $Z_0 = 120\pi$ Ω. From this data, the momentum relaxation time was determined to be ∼0.25 ps. This value is in good agreement with the momentum relaxation time determined from the transport measurements. Thus, in our hot electron bolometers, the Drude absorption provides a good coupling of THz radiation to 2-DEG up to 3 THz. Note that in AlGaN/GaN heterostructures, $\omega\tau = 4$ at 2.55 THz which is approximately 50 times smaller than that in a typical AlGaAs/GaAs heterostructure.

D. Thermal Characterization

For a bolometric detector, the photocurrent is proportional to $I \cdot dR/dT$, where I is the DC bias current, and *dR/dT* is the temperature coefficient of the 2-DEG resistance. To find the experimental value of the *dR/dT*, temperature dependence of 2-DEG resistance was measured between T = 77 K and T = 300 K. From the experimental data, we determined that *dR/dT* varies for different wafers from 3 Ω/K to 4 Ω/K at room temperature as it shown in Fig. 3. At temperature below 77 K, scattering on the lateral disordered potential is dominant. At temperatures above 100 K, the optical phonon scattering plays a greater role in the electron scattering processes [39], [40]. This provides a substantial sensitivity of the device resistance to the heating effects at high temperatures.

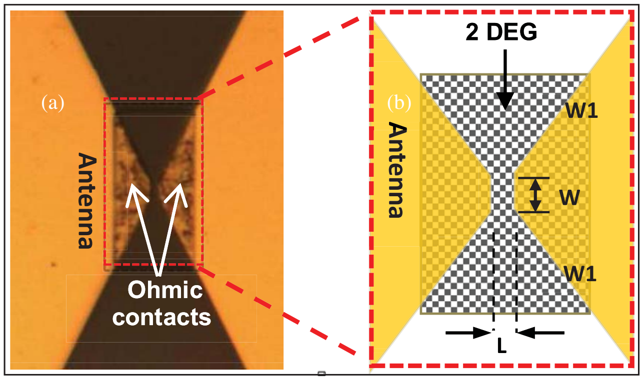

Fig. 4. (a) Image and (b) schematic of devices 1 and 2 with ohmic coupling. The apexes of the antenna and ohmic contacts have identical shapes. The ohmic contacts to 2-DEG are shown in dark color in (a) and (b).

III. Device Fabrication

The wafers were processed into the mesa structures by optical photolithography and dry etching in $SiCl_4$/Argon mixture plasma. A Ti/Al/Ti/Au metal stack of 25/70/50/100 nm thickness was deposited by e-beam evaporation after the etching process, and then the samples were annealed at 850 °C to form ohmic contacts [41]. The 2-DEG channel was located between the source and drain contacts and had different shape and dimensions for different devices.

An antenna made of 200 nm Ni/Au was deposited on the top of the ohmic contacts. The antennas were integrated with coplanar transmission lines designed for transmitting signals at an intermediate frequency. To reduce the electron heat capacity of the 2-DEG sensitive element (sensor), the area of the sensor, L × W, should be as small as possible. The effective aperture of an antenna, from which the antenna collects electromagnetic energy, is given by $A_{eff} = (g/\pi)\left(\lambda_{eff}/2\right)^2$ [42], where g is the antenna gain, λ_{eff} is the effective wavelength in the sapphire substrate, $\lambda_{eff} = \lambda_0/n_{eff}$, λ_0 is the wavelength in vacuum, $n_{eff} = \sqrt{(\varepsilon_r+1)/2}$, $\varepsilon_r \approx 10$ is the dielectric constant of sapphire. It is convenient to describe the efficiency of a micro-HEB integrated with the antenna by parameter $A_{eff}/(L\times W)$, which is proportional to $\lambda^2/(L\times W)$. This ratio has a simple physical sense: the antenna coupled to 2-DEG HEB collects the THz energy from the area of A_{eff} and delivers it to the 2-DEG spreading the energy over the area of L × W. The larger this parameter, the higher responsivity and sensitivity of the detector can be reached.

We designed two types of antenna-coupled HEBs with different coupling mechanisms. The first type is a traditional ohmic coupling between the 2-DEG and antenna via ohmic contacts, as it is illustrated in Figs. 4 and 5 for different types of antenna. However, the specific contact resistance of 300 Ω· μm prevents reduction of the width of the sensor below ~10 μm because it would lead to a large contact resistance (> 30 Ω).

To overcome this technological problem, we designed a 2-DEG micro-HEB with capacitive coupling between the 2-DEG sensor and antenna, which does not require fabrication of the ohmic contacts.

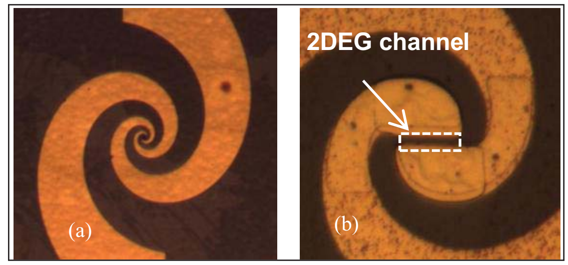

Fig. 5. (a) Image of device 3 with ohmic coupling. (b) Apexes of the spiral antenna form a 2 × 10 μm^2 2-DEG channel.

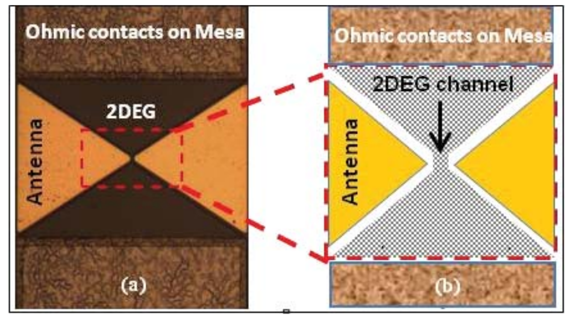

Fig. 6. (a) Image and (b) schematic of devices 4 with capacitive coupling. (b) Mesa is shaped in a form with narrow 8 × 4 μm^2 2-DEG channel between the apexes of the bow-tie antenna.

The capacitive coupling design and the corresponding device schematic are shown in Fig. 6. As it is seen from Fig. 6, there is no electrical connection between the antenna and the 2-DEG. The antenna is isolated from the 2-DEG in the same manner as the gate in a FET isolated from the 2-DEG channel. This design allows for employing the split-gate technique [43], [44] to control the 2-DEG channel length by the gate voltage and to decrease the sensor area down to 1 μm^2 and even below.

In this work, we designed and fabricated three types of broadband antennas covering a range of frequency from 1 THz to 4 THz: (i) a regular bow-tie, Fig. 4, (ii) a capacitive bow-tie, Fig. 6, and (iii) a spiral antenna shown in Fig. 5. The properties of these broadband antennas do not depend significantly on frequency over the frequency range of interest. Design of THz antennas is well established and optimized [42], [45]–[48]. The antennas have real impedance at the resonant frequency, while a deviation from the resonant frequency results in appearance of a capacitive component equal ~(10–30%) of the real component at the edge of the coverage [45]–[48]. To enhance the antenna gain, the devices were mounted on a reflective copper plate. The antenna parameters, such as antenna gain and impedance, are described in the next section.

IV. THz Photoresponse

The set-up for THz photocurrent measurements consists of a far-infrared gas laser FIRL-100 (Edinburgh Instruments) as the source of terahertz radiation, a low-noise SR-570 current preamplifier, a lock-in amplifier, and a chopper. In this work, the devices were exposed to THz radiation at a frequency of 2.55 THz. The photocurrent generated in a device was amplified by the preamplifier and registered by a lock-in amplifier. The gain of the preamplifier was 200 μA/V and the DC input impedance was 1 Ω. Since the laser operates in CW mode, a chopper was used to modulate the radiation incident on the device. The chopper frequency was used as the reference signal for the lock-in amplifier to get the high signal-to-noise ratio. A chopper frequency between 300 Hz and 1.3 kHz was used in the THz measurements in order to eliminate the low frequency electronic equipment noise and the effects associated with heating of the substrate, which are usually seen at frequencies below 300 Hz as it is shown in the following Subsection A. The HEBs were positioned directly into the laser beam at a distance of 50 cm from the laser output and aligned for a maximum response using the lock-in amplifier. A laser power density between 20 mW/cm^2 and 100 mW/cm^2 was sufficient to observe a reliable photoresponse without any focusing system. The responsivity of a HEB is defined as

$$R\left(\frac{mA}{W}\right) = \frac{I_{ph}\,(mA)}{A_{eff}\;P_L(W/cm^2)} \tag{2}$$

where I_{ph} is the photocurrent induced in the bolometer by the THz radiation, P_L is the power density of THz radiation; A_{eff} is the antenna effective aperture, introduced in the previous section.

A. Devices 1 and 2 With Ohmic Coupling

Device 1 has a mesa area of 40 $\times$ 40 μm^2 (marked by red dash line in Fig. 4a), and channel L $\times$ W = 2 $\times$ 2 μm^2 (see Fig. 4b). The flare angle of the antenna is 90°, the antenna impedance and gain are 80 Ω and 4.5 dB, correspondingly. Device 2 has similar geometry, but with twice as great mesa and channel: 40 $\times$ 80 μm^2 and L $\times$ W = 2 $\times$ 4 μm^2. The flare angle is 120°, the impedance is 60 Ω, and the antenna gain is 5 dB. The total DC resistance of device 1 and device 2 are 95 Ω and 55 Ω. The laser frequency was 2.55 THz, and its power density was 25 mW/cm^2, the chopper frequency was 1.3 kHz. Polarization of the THz radiation was the same as the direction of the bias current, between the ohmic contacts shown in Fig. 4b (horizontal polarization). The results of the measurements are shown in Fig. 7. As it is seen, the responsivity of device 1 reaches 15 mA/W at a bias of 10 mA. It is approximately 1.5 times greater than for device 2, which is in good agreement with the interpretation in terms of the parameter λ^2/(L$\times$W), discussed in section III, since the ratio of the areas of these devices equals two. The small difference can be accounted for the different antenna impedances. For the vertical polarization, the photoresponse is two times smaller because the bow-tie antenna does not operate for this polarization. For device 2, we also measured the dependence of the responsivity on the chopper modulation frequency. The result is shown in Fig. 8. As seen, at frequency above 300 Hz the low frequency electronic and/or thermal noise are suppressed.

B. Device 3

Device 3 integrated with a spiral antenna has also ohmic coupling between the antenna and 2-DEG. The device has a small mesa of 10 $\times$ 20 μm^2 and a narrow channel of 2 $\times$ 10 μm^2 as shown in Fig. 5. A broadband spiral antenna with an impedance of 60 Ω and gain 6 dB was fabricated over the ohmic contacts in the same manner as for device 1. We measured the photoresponse of this device at a frequency of 2.55 THz, a laser power of 58 mW/cm^2, and a chopper frequency of f = 1 kHz. As seen from Fig. 9, the THz response of this device is three times greater than the response of device 1 and reaches 40 mA/W at a bias current of 8 mA. It can be explained by the small areas of the mesa and channel in this device. To evaluate the sensitivity of the devices, we measured noise power produced by the bolometer sat a bias current of 2 mA and modulation frequency of 350 Hz and then calculated the optical noise-equivalent power (NEP) using the responsivity values determined above. The NEP was evaluated to beof ~5 nW/Hz$^{1/2}$ for our devices at 2.55 THz and room temperature.

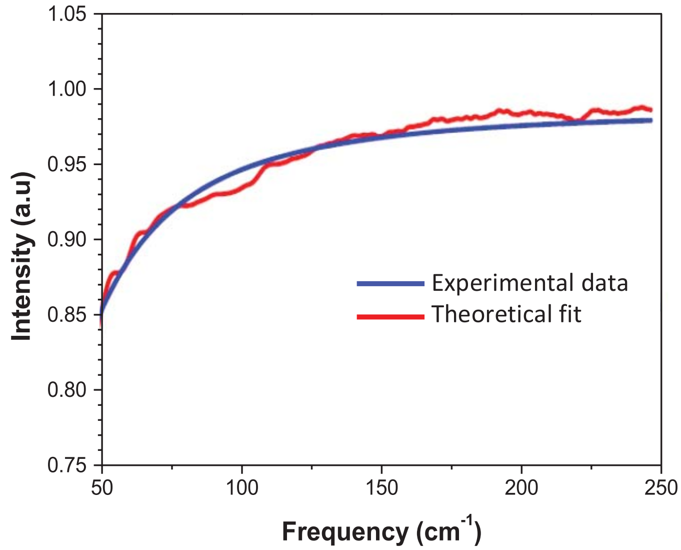

Fig. 7. Responsivity versus bias current for devices 1 and 2 with ohmic coupling between the antenna and 2-DEG.

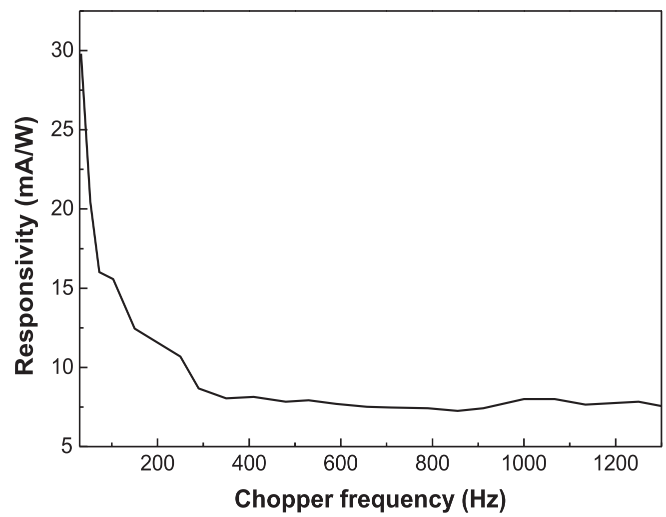

Fig. 8. Responsivity versus a chopper modulation frequency for device 2 at room temperature.

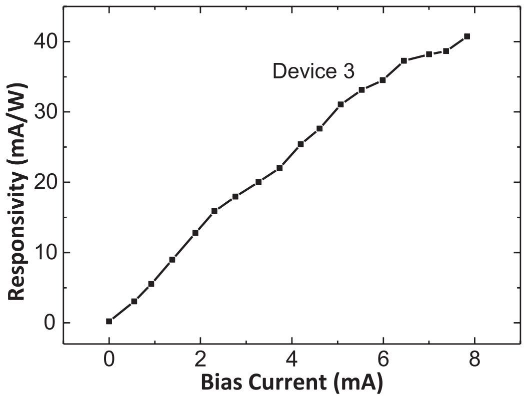

Fig. 9. Responsivity versus bias current for device 3 with ohmic coupling between the spiral antenna and 2-DEG.

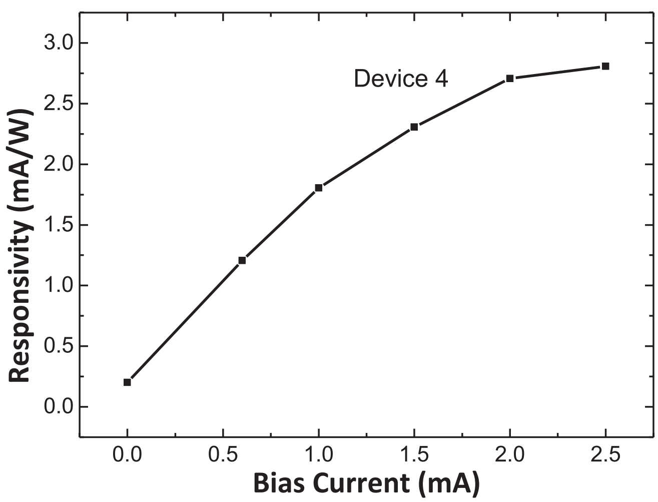

Fig. 10. Responsivity versus bias current for device 4 with capacitive between coupling the bow-tie antenna and 2-DEG.

C. Capacitive Coupling

In device 4, the 2-DEG channel is not directly connected to the bow-tie antenna terminals, see Fig. 6. The device operation is based on the capacitive coupling between the antenna and 2-DEG. The mesa is shaped in such a way that it tapers from the contact sides towards the antenna terminals, as it shown in Fig. 6b. The narrow 2 μm × 4 μm channel is positioned between the bow-tie antenna apexes. The THz electric field induced in the gap between antenna apexes heats the 2-DEG in the channel. With a flare angle of 60°, the antenna has an impedance of 85 Ω, a gain of 5 dB, and the DC resistance of the device is 1.9 kΩ. The following experimental settings were chosen for the measurement of this device: the laser frequency was 2.55 THz, the laser power was 50 mW/cm^2, and the chopping frequency was 355 Hz. The result of the room temperature measurement is shown in Fig. 10 for the horizontal polarization. For the vertical polarization, the photoresponse is 1.5 times smaller compared with a case of the horizontal polarization. For the vertical polarization, the antenna does not contribute to heating of 2-DEG. However, the 2-DEG sensor by itself may operate as an antenna [49], because the 2-DEG layer has a shape of the bow-tie antenna with a flare angle of 120°.

As it is seen from Fig. 10, the response of device 4 with capacitive coupling is similar to those shown in Fig. 7 at low bias current, but it is significantly less than for device 3. For device 4, the NEP was evaluated as ∼8 nW/Hz$^{1/2}$ at a bias current of 1 mA and modulation frequency of 355 Hz.

Summarizing the results of Section IV, we can notice that the experimental data confirm that the photoresponse is proportional to the ratio A_{eff}/(L×W), as expected for our quasi-optical setup.

V. Conclusion

We have designed, fabricated, and tested 2-DEG THz hot-electron bolometers based on low-mobility AlGaN/GaN heterostructures. We demonstrated the room temperature operation of these devices at 2.55 THz with the responsivity up to ∼0.04 A/W and NEP ∼5 nW/Hz$^{1/2}$. This responsivity has been achieved due to the strong Drude absorption, low dimensionality of the electron subsystem, a small area of the 2-DEG sensor, and a low resistance of the ohmic contacts. We also demonstrated successful operation of the devices with capacitive (contact less, non-ohmic) coupling between the 2-DEG sensor and THz antenna.

Responsivity and NEP of our devices can be compared with the recently reported R = 0.07 A/W and NEP ∼40 pW/Hz$^{1/2}$ achieved in a 2-DEG GaN-based FET at 950 GHz [50], [51]. A ten times greater responsivity (0.5 A/W) was observed at 3.7 K with a quantum well THz detector [52]. Shuster et al. [53] demonstrated recently a FET THz detector with a NEP of 10 pW/Hz$^{1/2}$ at 300 GHz at room temperature. Authors of [54], [55] report on THz detection by YBCO high-T_c super conductor bolometers operating at 77 K with a NEP of 20 pW/Hz$^{1/2}$ at 1.6 THz and NEP of 3.5 nW/Hz$^{1/2}$ at 2.5 THz.

The NEP value 5 nW/Hz$^{1/2}$ demonstrated by our devices is higher than the theoretical limit ∼10 pW/Hz$^{1/2}$ for these devices at room temperature. Our analysis shows that the responsivity and NEP of our devices can be significantly improved by 1) further reduction the sensor area, 2) growing GaN structures with a lower electron mobility, and 3) increasing the coupling between the antenna and 2-DEG sensor. The devices with the capacitive coupling look promising for realization of these improvements.

Acknowledgment

The authors would like to thank Dr. R. Gaska and Dr. D. Billingsley for growing the GaN wafers.

References

[1] A. Rogalski and F. Sizov, "Terahertz detectors and focal plane arrays," *Opto-Electron. Rev.*, vol. 19, no. 3, pp. 346–404, Sep. 2011.

[2] K. Shibata, A. Umeno, K. M. Cha, and K. Hirakawa, "Photon-assisted tunneling through self-assembled InAs quantum dots in the terahertz frequency range," *Phys. Rev. Lett.*, vol. 109, no. 7, pp. 077401-1–077401-5, Aug. 2012.

[3] M. S. Vitiello, D. Coquillat, L. Viti, D. Ercolani, F. Teppe, A. Pitanti, F. Beltram, L. Sorba, W. Knap, and A. Tredicucci, "Room-temperature terahertz detectors based on semiconductor nanowire field-effect transistors," *Nano Lett.*, vol. 12, no. 1, pp. 96–101, Dec. 2012.

[4] T. Zhou, R. Zhang, X. G. Guo, Z. Y. Tan, Z. Chen, J. C. Cao, and H. C. Liu, "Terahertz imaging with quantum-well photodetectors," *IEEE Photon. Technol. Lett.*, vol. 24, no. 13, pp. 1109–1111, Jul. 2012.

[5] M. Rinzan, G. Jenkins, H. D. Drew, S. Shafranjuk, and P. Barbara, "Carbon nanotube quantum dots as highly sensitive terahertz-cooled spectrometers," *Nano Lett.*, vol. 12, no. 6, pp. 3097–3100, May 2012.

[6] L. Vicarelli, M. S. Vitiello, D. Coquillat, A. Lombardo, A. C. Ferrari, W. Knap, M. Polini, V. Pellegrini, and A. Tredicucci, "Graphene field effect transistors as room-temperature terahertz detectors," *Nature Mater.*, vol. 11, pp. 865–871, Mar. 2012.

[7] V. Ryzhii and M. Ryzhii, "Graphene bilayer field-effect phototransistor for terahertz and infrared detection," *Phys. Rev. B*, vol. 79, no. 24, pp. 245311-1–245311–8, Jun. 2009.

[8] M. E. Itkis, F. Borondics, A. Yu, and R. C. Haddon, "Bolometric infrared photoresponse of suspended single-walled carbon nanotube films," *Science*, vol. 312, no. 5772, pp. 413–421, Apr. 2006.

[9] J. Wei, D. Olaya, B. S. Karasik, S. V. Pereverzev, A. V. Sergeev, and M. E. Gershenson, "Ultrasensitive hot-electron nanobolometers for terahertz astrophysics," *Nature Nanotechnol.*, vol. 3, pp. 496–500, Jul. 2008.

[10] B. Karasik and A. Sergeev, "THz hot-electron photon counter," *IEEE Trans. Appl. Superconduct.*, vol. 15, no. 2, pp. 618–621, Jun. 2005.

[11] D. Mittleman, *Sensing with Terahertz Radiation*. New York: Springer-Verlag, 2002.

[12] D. Van der Weide, "Applications and outlook for electronic terahertz technology," *Opt. Photon. News*, vol. 14, no. 4, pp. 48–53, 2003.

[13] M. Tonouchi, "Cutting-edge terahertz technology," *Nature Photon.*, vol. 1, pp. 97–105, Dec. 2007.

[14] T. Crowe, R. Mattauch, H. Roser, W. Bishop, W. Peatman, and X. Liu, "GaAs Schottky diodes for THz mixing applications," *Proc. IEEE*, vol. 80, no. 11, pp. 1827–1841, Nov. 1992.

[15] H. P. Röser, H. W. Hübers, T. W. Crowe, and W. C. B. Peatman, "Nanostructure GaAs Schottky diodes for far-infrared heterodyne receivers," *Infr. Phys. Technol.*, vol. 35, nos. 2–3, pp. 451–462, Mar.–Apr. 1994.

[16] P. H. Siegel, "Terahertz technology," *IEEE Trans. Microw. Theory Tech.*, vol. 50, no. 3, pp. 910–928, Mar. 2002.

[17] H. Ekström and B. Karasik, "Electron temperature fluctuation noise in hot-electron superconducting mixers," *Appl. Phys. Lett.*, vol. 66, no. 23, pp. 3212–3214, Jun. 1995.

[18] I. Siddiqi, A. Verevkin, D. E. Prober, A. Skalare, W. R. McGrath, P. M. Echternach, and H. G. LeDuc, "Heterodyne mixing in diffusion-cooled superconducting aluminum hot-electron bolometers," *J. Appl. Phys.*, vol. 91, no. 7, pp. 4646–4654, Apr. 2002.

[19] S. Cherednichenko, V. Drakinskiy, J. Baubert, J.-M. Krieg, B. Voronov, G. Goltsman, and V. Desmaris, "Gain bandwidth of NbN hot-electron bolometer terahertz mixers on 1.5 μm Si_3N_4/SiO_2 membranes," *J. Appl. Phys.*, vol. 101, no. 12, pp. 124508-1–124508-6, Jun. 2007.

[20] B. S. Karasik, W. R. McGrath, and M. C. Gaidis, "Analysis of a high-Tc hot-electron superconducting mixer for terahertz applications," *J. Appl. Phys.*, vol. 81, no. 2, pp. 1581–1589, Jun. 1997.

[21] B. S. Williams, "Terahertz quantum-cascade lasers," *Nature Photon.*, vol. 1, pp. 517–525, Jul. 2007.

[22] M. A. Belkin, F. Capasso, A. Belyanin, D. L. Sivco, A. Y. Cho, D. C. Oakley, C. J. Vineis, and G. W. Turner, "Terahertz quantum-cascade-laser source based on intracavity difference-frequency generation," *Nature Photon.*, vol. 1, pp. 288–294, Jul. 2007.

[23] M. C. Wanke, E. W. Young, C. D. Nordquist, M. J. Cich, A. D. Grine, C. T. Fuller, J. L. Reno, and M. Lee, "Monolithically integrated solid-state terahertz transceivers," *Nature Photon.*, vol. 4, pp. 565–569, Jun. 2010.

[24] J. X. Yang, F. Agahi, D. Dai, C. F. Musante, W. Grammer, K. M. Lau, and K. S. Yngvesson, "Wide-bandwidth electron bolometric mixers: A 2DEG prototype and potential for low noise THz receivers," *IEEE Trans. Microw. Theory Tech.*, vol. 41, no. 4, pp. 581–589, Apr. 1993.

[25] K. S. Yngvesson, "Ultrafast two-dimensional electron gas detector and mixer for terahertz radiation," *Appl. Phys. Lett.*, vol. 76, no. 6, pp. 777–779, Feb. 2000.

[26] M. Lee, L. N. Pfeiffer, K. W. West, and K. W. Baldwin, "Wide bandwidth millimeter wave mixer using a diffusion cooled two-dimensional electron gas," *Appl. Phys. Lett.*, vol. 78, no. 19, pp. 19–21, 2001.

[27] M. Lee, L. N. Pfeiffer, and K. W. West, "Ballistic cooling in a wideband two-dimensional electron gas bolometric mixer," *Appl. Phys. Lett.*, vol. 81, no. 7, pp. 1243–1245, 2002.

[28] T. Otsuji, M. Hanabe, and O. Ogawara, "Terahertz plasma wave resonance of two-dimensional electrons in InGaP/InGaAs/GaAs high-electron-mobility transistors," *Appl. Phys. Lett.*, vol. 85, no. 11, pp. 2119–2121, 2004.

[29] V. Ryzhii, I. Khmyrova, and M. Shur, "Terahertz photomixing in quantum well structures using resonant excitation of plasma oscillations," *J. Appl. Phys.*, vol. 91, no. 4, pp. 1875–1881, 2002.

[30] A. V. Muravjov, D. B. Veksler, V. V. Popov, O. V. Polischuk, N. Pala, X. Hu, R. Gaska, H. Saxena, R. E. Peale, M. S. Shur, "Temperature dependence of plasmonic terahertz absorption in grating-gate gallium-nitride transistor structures," *Appl. Phys. Lett.*, vol. 96, no. 4, pp. 042105-1–042105-3, 2010.

[31] R. Ramaswamy, K. Wang, A. Stier, A. Muraviev, G. Strasser, A. Markelz, M. Shur, R. Gaska, A. Sergeev and V. Mitin, "2DEG GaN hot electron microbolometers and quantum cascade lasers for THz heterodyne sensing," *Proc. SPIE, Micro-Nanotechnol. Sensors, Syst., Appl. III*, vol. 8031, p. 80310H, May 13, 2011, doi:10.1117/12.883329.

[32] A. Sergeev, M. Y. Reizer, and V. Mitin, "Deformation electron-phonon coupling in disordered semiconductors and nanostructures," *Phys. Rev. Lett.*, vol. 94, no. 13, pp. 136602-1–136602-4, 2005.

[33] M.Gonschorek, J.F. Carlin, E.Feltin, M. A. Py, N. Grandjean, V.Darakchieva, B. Monemar, M. Lorenz, and G. Ramm, "Two-dimensional electron gas density in $Al_{1-x}In_xN$/AlN/GaN heterostructures ($0.03 \le x \le 0.23$)," *J. Appl. Phys.*, vol. 103, no. 9, pp. 093714–093720, 2008.

[34] Y. Cao and D. Jena, " High-mobility window for two-dimensional electron gases at ultrathin AlN/GaN heterojunctions," *Appl. Phys. Lett.*, vol. 90, no. 18, pp. 182112–182114, 2007.

[35] R. Tülek, A. Ilgaz, S. Gökden, A. Teke, M. K. Öztürk, M. Kasap, S. Özçelik, E. Arslan, and E. Özbay, "Comparison of the transport properties of high quality AlGaN/AlN/GaN and AlInN/AlN/GaN two-dimensional electron gas heterostructures," *J. Appl. Phys.*, vol. 105, no. 1, pp. 013707–013716, 2009.

[36] Y. Hao, L. A. Yang, and J. C. Zhang, "GaN-based semiconductor devices for terahertz technology," *Terahertz Sci. Technol.*, vol. 1, no. 2, pp. 51–64, Jun. 2008.

[37] O. Ambacher, J. Smart, J. R. Shealy, N. G. Weimann, K. Chu, M. Murphy, W. J. Schaff, L. F. Eastman, R. Dimitrov, L. Wittmer, M. Stutzmann, W. Rieger, and J. Hilsenbeck, "Two-dimensional electron gases induced by spontaneous and piezoelectric polarization charges in N- and Ga-face AlGaN/GaN heterostructures," *J. Appl. Phys.*, vol. 85, no. 6, pp. 3222–3233, 1999.

[38] N. A. Kabir, Y. Yoon, J. R. Knab, J. Y. Chen, A. G. Markelz, J. L. Reno, Y. Sadofyev, S. Johnson, Y.-H. Zhang, and J. P. Bird, "Terahertz transmission characteristics of high-mobility GaAs and InAs two-dimensional-electron-gas systems," *Appl. Phys. Lett.*, vol. 89, no. 13, pp. 132109–132111, 2006.

[39] A. Matulionis, J. Liberis, E. Šermukšnis, J. Xie, J. H. Leach, M. Wu, and H. Morkoç, "Hot-electron energy relaxation time in AlInN/AlN/GaN 2DEG channels," *Semicond. Sci. Technol.*, vol. 23, no. 7, pp. 075048-1–075048-6, 2008.

[40] F. G. Bass and V. A. Pogrebnyak, "Hot electron scattering by localized optical modes in a polar semiconductor," *Solid State Commun.*, vol. 85, no. 1, pp. 32–34, 1993.

[41] A. N. Bright, P. J. Thomas, M. Weyland, D. M. Tricker, and C. J. Humphreys, "Correlation of contact resistance with microstructure for Au/Ni/Al/Ti/AlGaN/GaN ohmic contacts using transmission electron microscopy," *J. Appl. Phys.*, vol. 89, no. 6, pp. 3143–3150, 2001.

[42] C. Balanis, *Antenna Theory*, 3rd ed. New York: Wiley, 2005.

[43] M. Bell, A. Sergeev, J. Bird, V. Mitin, and A. Verevkin, "Crossover from Fermi liquid to multichannel Luttinger liquid in high-mobility quantum wires," *Phys. Rev. Lett.*, vol. 104, no. 4, pp. 046805-1–046805-4, 2010.

[44] T. Sugaya, J. P. Bird, D. K. Ferry, A. Sergeev, V. Mitin, K.-Y. Yang, M. Ogura, and Y. Sugiyama, "Experimental studies of the electron–phonon interaction in InGaAs quantum wires," *Appl. Phys. Lett*, vol. 81, no. 4, pp. 727–730, 2002.

[45] J. L. Volakis, *Antenna Engineering Handbook*, 4th ed. New York: McGraw-Hill, 2007.

[46] R. Compton, R. McPhedran, Z. Popovic, G. Rebeiz, P. Tong, and D. Rutledge, "Bow-tie antennas on a dielectric half-space: Theory and experiment," *IEEE Trans. Antennas Propagat.*, vol. 35, no. 6, pp. 622–631, Jun. 1987.

[47] A. D. Semenov, H. Richter, H. W. Hübers, B. Günther, A. Smirnov, K. S. Il'in, M. Siegel, and J. P. Karamarkovic, "Terahertz performance of integrated lens antennas with a hot-electron bolometer," *IEEE Trans. Microw. Theory Tech.*, vol. 55, no. 2, pp. 239–247, Feb. 2007.

[48] J. H. Kim, C. G. Christodoulou, Z. Ku, Y. C. Xin, N. A. Naderi, and L. F. Lester, "Quantum-dot laser coupled bow-tie antenna," in *Proc. IEEE Int. Symp. Antennas Propagat. Soc.*, San Diego, CA, Mar. 2008, pp. 1–4.

[49] D. Seliuta, E. Sirmulis, V. Tamosiunas, S. Balakauskas, S. Asmontas, A. Suziedelis, J. Gradauskas, G. Valusis, A. Lisauskas, and K. Kohler, "Detection of terahertz/sub-terahertz radiation by symmetrically shaped 2DEG layers," *Electron. Lett.*, vol. 40, no. 10, pp. 631–632, 2004.

[50] J. D. Sun, Y. F. Sun, D. M. Wu, Y. Cai, H. Qin, amd B. S. Zhang, "High-responsivity, low-noise, room-temperature, self-mixing terahertz detector realized using floating antennas on a GaN-based field-effect transistor," *Appl. Phys. Lett.*, vol. 100, no. 1, pp. 013506-1–013506-3, 2012.

[51] Y. F. Sun, J. D. Sun, Y. Zhou, R. B. Tan, C. H. Zeng, W. Xue, H. Qin, B. S. Zhang, and D. M. Wu, "Room temperature GaN/AlGaN self-mixing terahertz detector enhanced by resonant antennas," *Appl. Phys. Lett.*, vol. 98, no. 25, pp. 252103-1–252103-3, 2011.

[52] T. Zhou, R. Zhang, X. G. Guo, Z. Y. Tan, Z. Chen, J. C. Cao, and H. C. Liu, "Terahertz imaging with quantum-well photodetectors," *IEEE Photon. Technol. Lett.*, vol. 24, no. 13, pp. 1109–1111, Jul. 2012.

[53] F. Schuster, D. Coquillat, H. Videlier, M. Sakowicz, F. Teppe, L. Dussopt, B. Giffard, T. Skotnicki, and W. Knap, "Broadband terahertz imaging with highly sensitive silicon CMOS detectors," *Opt. Exp.*, vol. 19, no. 8, pp. 7827–7832, 2011.

[54] A. Hammar, S. Cherednichenko, S. Bevilacqua, V. Drakinskiy, and J. Stake, "Terahertz direct detection in $YBa_2Cu_3O_7$ microbolometers," *IEEE Trans. Terahertz Sci. Technol.*, vol. 1, no. 2, pp. 390–394, Nov. 2011.

[55] A. V. Smirnov, M. S. Karmantsev, K. B. Smirnov, Y. B. Vakhtomin, D. V. Masterov, M. A. Tarkhanov, S. A. Pavlov, and A. E. Parafin, "THz bolometer based on a thin YBCO film," *Zhurnal Tekh. Fiziki*, vol. 82, pp. 108–111, Feb. 2012.

Jae Kyu Choi received the B.S. degree in physics from Kyung Hee University, Seoul, Korea, in 2001, where he received the M.Sc. degree in physics in collaboration with the Korea Institute of Science and Technology, Seoul, in 2003. His thesis work was focused on the study of photoluminescence in nanocrystalline Si (nc-Si). He is currently pursuing the Ph.D. degree in Physics with University at Buffalo, The State University of New York, Buffalo, NY.

He was a full-time Lecturer of physics with the Naval Academy, Jinhae, Korea, during his military service from 2003 to 2006. His current research interests include 2DEG hot-electron microbolometers for THz heterodyne sensing, and remote temperature sensing using voltage-tunable multicolor QWIPs.

Vladimir Mitin (F'11) received the Doctor of Science degree from the Institute of Semiconductors, Ukrainian Academy of Sciences, Kiev, Ukraine, in 1987.

He is currently a SUNY Distinguished Professor with the Department of Electrical Engineering, University at Buffalo, The State University of New York, Buffalo, NY. He has authored or co-authored more than 500 papers in journals and conferences, four monographs, and five textbooks. He holds ten patents. His publications have been cited more than 1500 times, and his h-index is 19. His current interests include nanoelectronic, microelectronic, and optoelectronic devices, and materials with special emphasis on sensors and detectors based on nanostructures.

Dr. Mitin is a fellow of the AAAS and IoP.

Rahul Ramaswamy was born in Bangalore, India, on March 19, 1984. He received the B.S. degree from the Department of Electronics and Communications, Vemana Institute of Technology, Bangalore, in 2006, the M.S. degree from the Electrical Engineering Department, University at Buffalo (UB), The State University of New York, Buffalo, NY, in 2009. His M.S. thesis was focused on characterization of 2DEG microbolometers for mixing at millimeter and submillimeter wavelengths. He received the Ph.D. degree from UB in 2011. His Ph.D. thesis was focused on hot-electron GaN 2DEG microbolometers for advanced THz spectroscopy.

He is currently with Intel Corporation, Portland, OR, as a Process Integration Engineer.

Victor A. Pogrebnyak received the Doctor of Science degree in solid-state physics from the Institute for Radio-Physics and Electronics (IRE), Kharkov, Ukraine, and the University of Latvia, Riga, Latvia, in 1991.

He was a Senior Scientist at IRE from 1982 to 1998. From 1999 to 2006, he was a Professor with the Department of Electrical Engineering, Çukurova University, Adana, Turkey. He joined the Department of Electrical Engineering, University at Buffalo, The State University of New York, Buffalo, NY, as an Adjunct Associate Professor, Lecturer, and Scientist, in 2007. He has authored or co-authored more than 100 papers in journals and conferences. His current research interests include microwaves, THz, and infrared detectors, hot-electron devices, quantum transport in nanostructures, and wave propagation in periodic structures.

Mehdi Pakmehr received the B.S. degree in theoretical physics from the University of Tabriz, Tabriz, Iran, in 2007, and the M.S. degree in physics, specializing in metamaterials, from the University at Buffalo, Buffalo, NY, in 2011, where he is currently pursuing the Ph.D. degree with the Far Infrared Magneto-Spectroscopy Laboratory, Department of Physics.

His research focuses on THz spectroscopy of nanostructures, specifically cyclotron resonance and electron spin resonance in two-dimensional electron gases (2DEGs) and quantum wires. He has developed an analysis method for THz magnetophotoresponse measurements, which can be used to characterize 2DEGs formed in different systems like quantum wells, graphene, and surface electrons in topological insulators.

Andrey Muraviev (native spelling Muravjov) received the Ph.D. degree in physics from the Institute of Applied Physics, Russian Academy of Sciences, Nizhny Novgorod, Russia, in 1992.

He was a Senior Research Scientist with the Institute for Physics of Microstructures, Russian Academy of Sciences, where he was engaged in research on development of p-Ge terahertz semiconductor lasers. Since 1997, he has been a Visiting Research Scientist with the University of Central Florida, Orlando, Rensselaer Polytechnic Institute, Troy, NY, and University at Buffalo, The State University of New York, Buffalo, NY, on terahertz-related projects. He has authored or co-authored over 70 papers in refereed journals and conferences. His current research interests include THz semiconductor lasers and detectors, THz and mid-IR spectroscopy.

Michael S. Shur (F'89–LF'09) is currently a Roberts Professor and the Acting Director of the Center for Integrated Electronics, Rensselaer Polytechnic Institute, Troy, NY.

Dr. Shur was a recipient of the Tibbetts Award for Technology Commercialization, the St. Petersburg Technical University Honorary Doctorate, the IEEE Kirchmayer Award, the Gold Medal of Russian Education Ministry, and Best Paper Awards. He is a Foreign Member of the Lithuanian Academy of Sciences. He is a Life Fellow of the APS and SPIE, a fellow of OSA, IET, ECS, WIF, MRS, AAAS, Sigma Xi, and Humboldt Societies, and a member of Eta Kappa Nu, Tau Beta Pi, ASEE. He is the Editor-in-Chief of IJHSES, the Vice-President of the IEEE Sensors Council, and a Distinguished Lecturer of the IEEE EDS. He is a Co-Founder and the Vice-President of Sensor Electronics Technology, Inc.

John J. Gill received the B.S. and M.S. degrees in mechanical engineering from the University of California, Los Angeles, in 1997, where he received the Ph.D. degree in microelectromechanical systems in 2001.

He was with Jet Propulsion Laboratory (JPL), Pasadena, CA, from 1997 to 1998, where he was involved in development of quantum-well-infrared-photodetectors. Since 2001, he has been with JPL, where he has been mainly involved in the Herschel Project as a Team Leader who is in charge of manufacturing and delivering high-quality GaAs Schottky diode multipliers and mixers for submillimeter and microwave applications. His current research interests include design, fabrication, and characterization of microelectronic devices based on silicon, III–V, and II–VI materials for space and industry applications.

Imran Mehdi (S'85–M'91–SM'05–F'09) received the Certificate in Letters and Science from Calvin College, Grand Rapids, MI, in 1983, and the B.S.E.E., M.S.E.E., and Ph.D.(E.E.) degrees from the University of Michigan, Ann Arbor, in 1984, 1985, and 1990, respectively.

He joined the Jet Propulsion Laboratory, California Institute of Technology, Pasadena, in 1990, where he was involved in the design and fabrication of planar Schottky diodes that have been deployed in several space instruments, including the Aura spacecraft and the Herschel Space Observatory—a cornerstone European Space Agency mission. He is currently a Senior Research Scientist and the Group Supervisor of the Submillimeter-Wave Advanced Technology Group, Jet Propulsion Laboratory, California Institute of Technology, Pasadena, where he is engaged in developing THz technology for future NASA missions. His current research interests include submillimeter-wave devices, instrumentation, and heterodyne receivers.

Boris S. Karasik (M'11) received the B.S. degree from Petrozavodsk State University, Petrozavodsk, Russia, in 1979, and the Ph.D. degree from Moscow State Pedagogical University, Moscow, Russia, in 1979 and 1988, respectively, both in physics.

He participated in many Russian, U.S., and European projects on hot-electron device physics and applications. He joined the Jet Propulsion Laboratory (JPL), California Institute of Technology, Pasadena, in 1995, as a Member of Technical Staff, where he is currently a Principal Research Technologist. He has authored or co-authored over 135 journal and conference papers and holds six patents.

Dr. Karasik was a recipient of several NASA and JPL awards and certificates of recognition for technical achievements. He is a member of the American Physical Society, SPIE, and Sigma Xi.

Andrei V. Sergeev received the B.S. and M.S. degrees in physics from the Moscow Institute of Physics and Technology, Moscow, Russia, in 1978 and 1980, respectively, and the Ph.D. degree in theoretical solid-state physics from Moscow State Pedagogical University, Moscow, in 1987.

He is currently with the University at Buffalo, The State University of New York, Buffalo, where he conducts research on various topics, including hot-electron nanodetectors, single-photon counters, nanocalorimeters, wide-band mixers, quantum-dot detectors, and solar cells. His design of advanced devices is based on multiscale modeling, which includes quantum transport, hydrodynamic transport, and Monte-Carlo simulations. He has authored or co-authored more than 100 scientific papers in refereed journals. His current research interests include quantum kinetics and transport in nanostructures, and modeling of nanodevices and nanosensors.